Bulletin of the Seismological Society of America, Vol. 93, No. 2, pp. 546–556, April 2003

Soil-Structure Interaction and Site Response at the Jensen Filtration Plant during the 1994 Northridge, California, Mainshock and Aftershocks

by C. B. Crouse and Juan Carlos Ramirez

Abstract The effects of soil-structure interaction (SSI) and nonlinear site response (SR) on the Northridge mainshock and aftershock motions recorded at two buildings in the Jensen Filtration Plant were investigated. Forced vibration tests conducted on the small one-story generator building and the larger three-story administration building, both of which recorded the mainshock and two aftershock sequences, revealed a prominent mode of vibration at 6.2 Hz in the short (east–west) direction of the administration building. However, models of inertial SSI, calibrated to the vibration-test data, demonstrated that this phenomenon was of secondary importance, even when adjusted for nonlinear behavior of the soil and structure. Nonlinear SR and kinematic SSI were identified as the main reasons for the differences observed in the three sets of building earthquake records, each with clearly distinct amplitude and duration characteristics. Unfortunately, the absence of free-field recordings at both buildings during the mainshock and first aftershock sequence prevented a clearer determination of the relative roles of these two phenomena. Fortunately, the installation of free-field instruments outside both buildings 4 yr later revealed the significance of both effects, albeit at extremely small motion amplitudes. This case history further emphasizes the need to carefully plan the siting of ground-motion instrumentation so that the interpretations of any recorded data are not obscured by the potential effects of SSI.

Introduction

This study extends the previous investigation of Cultrera *et al.* (1999) in an attempt to more clearly identify the relative contributions of soil-structure interaction (SSI) and nonlinear site response (SR) to the motions recorded at two sites within the Jensen Filtration Plant (JFP) during the 1994 Northridge mainshock and two aftershock sequences. The moment magnitude **M** 6.7 mainshock and six aftershocks within the ensuing 24-hr period were recorded in the bottom level (designated as first floor in this study and as basement in Cultrera *et al.*) of a three-story administration building (subsequently designated as JAB) and on the ground floor of a small one-story generator building (JGB) (Fig. 1). These events are identified as MS (mainshock) and AS1, AS2, AS3, AS4, AS6, and AS7 (AS5 was not recorded at JFP) in table 3 of Cultrera *et al.* (1999), which presents relevant information on the hypocentral locations of these and subsequent events, as well as the peak ground motions recorded at both buildings. Almost 4 yr after the main shock, GEOS recorders were collocated next to the accelerographs inside the buildings, and another pair of these instruments were located at free-field sites nearby. In a 2-month period these instruments recorded seven aftershocks (5 to 11 in table 3 of Cultrera *et al.* 1999). These referenced recordings from the mainshock (MS), initial aftershocks (AS), and latter aftershocks (GEOS) constitute the dataset analyzed by Cultrera *et al.* and in this study. However, each study treated the data differently in one potentially important respect. Cultrera *et al.* took the geometric mean of the Fourier amplitude spectra of both horizontal components of each record, whereas this study considered the components separately because of potential influences of inertial SSI, which was found to be different in the short (east–west) and long (north–south) directions of the JAB.

This article first summarizes the relevant aspects of the JAB and JGB buildings and their site geologies. Next, the results of forced vibration tests on both buildings are presented, followed by the calibration of inertial SSI models and development of corresponding theoretical transfer functions between the motions at both sites and both buildings. Finally, modifications to the building transfer functions are introduced to account for kinematic SSI, which is the filtering of high-frequency motions by the building foundations. The various theoretical and empirical transfer functions are compared to deduce the roles of SSI and site response at small and large amplitudes of motion.

All transfer functions presented in this report show the

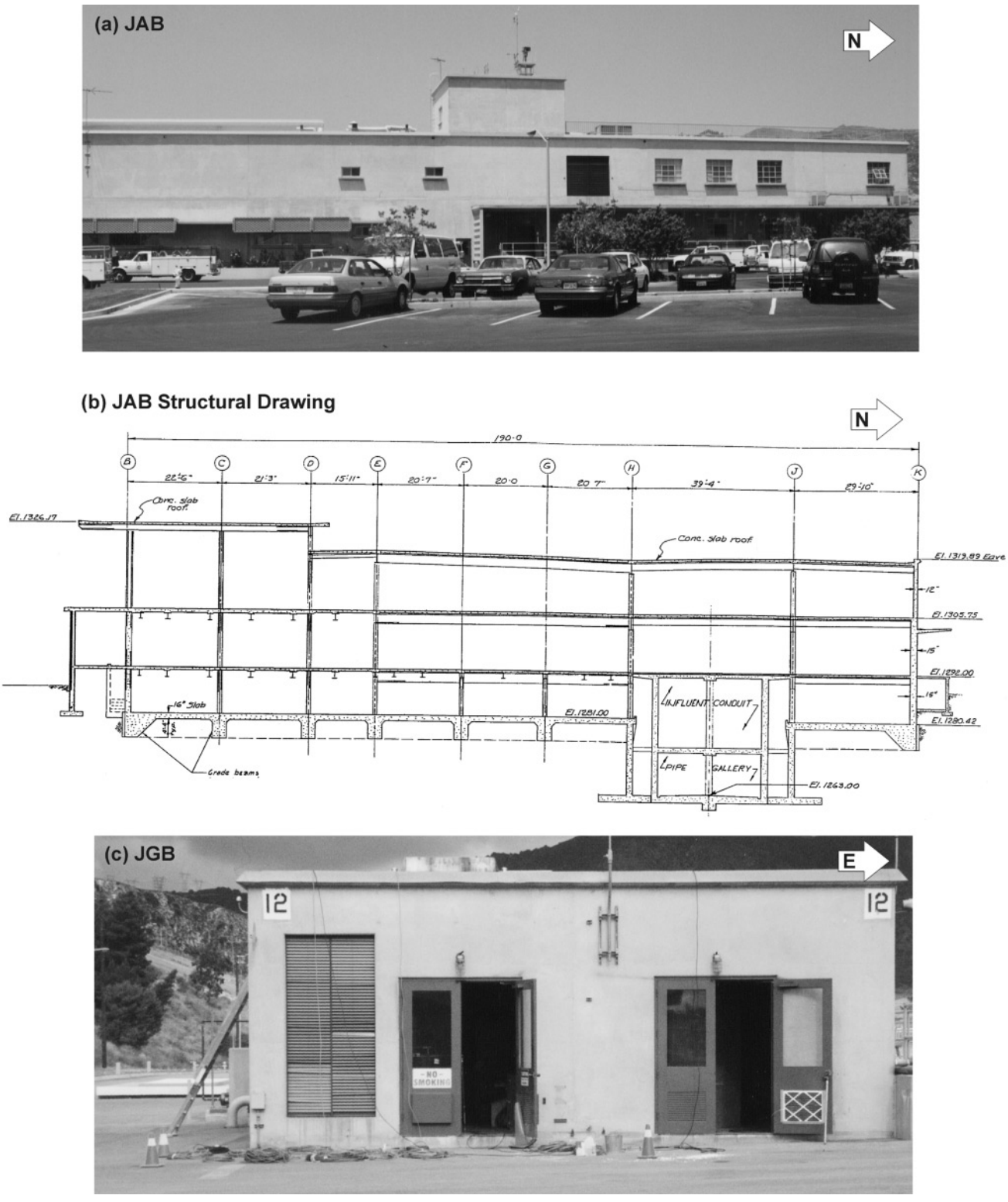

Figure 1. Jensen Filtration Plant buildings: (a) view of east side (long direction) of JAB, (b) structural drawing of JAB (view from same direction as photo) with elevation in feet and dimensions in feet and inches (12″ = 1′ = 0.305 m), (c) view of south side of JGB.

amplitude ratios versus frequency for either (1) the base level to free-field motions at the JAB or JGB, or (2) the base-level (or free-field) motions at JAB to the base-level (or free-field) motions at JGB.

Building and Site Information

The JAB is a three-story exterior reinforced concrete (RC) and interior steel-frame building with the first floor (elevations 1280.42 and 1281.00 in Fig. 1b) embedded about 3 m below grade and supported on a 0.41-m-thick RC slab cast monolithically with underlying grade beams. The plan dimensions of the building are 58 m × 28 m. A picture showing most of the longitudinal length of the building is presented in Figure 1a. A large east–west oriented conduit structure (Fig. 1b) runs through the lower portion of the north end of the building. In contrast, the JGB is a one-story RC slab-on-grade structure (Fig. 1c) with a basement beneath the eastern one-half of the building. The plan dimensions of this building at grade level are 10.1 m × 9.6 m.

The strong-motion accelerograph in the JAB is at the embedded first-floor level, while the accelerograph in the JGB is on the ground-level floor slab.

The distance between the buildings is approximately 260 m. The principal horizontal directions of the buildings are parallel, and the long direction of the JAB is N22° E, which will subsequently be referenced as the NS direction. Aside from the structural differences between the two buildings, the surficial geologies at the two sites are also different. The JGB site consists of a thin (3 m thick) layer of engineered fill whereas the JAB site consists of approximately 14 m of engineered fill and native sandy soil. At both sites these materials are underlain by the Plio-Pleistocene Saugus formation, which consists of sandstone, siltstone, and claystone (Gibbs *et al.*, 1999). The shear-wave velocities (V_s) measured near each building indicate that the fill at the JGB site is much stiffer ($V_s \sim 350$ to 400 m/sec) than the fill/alluvium at the JAB site, which has a $V_s \sim 250$ to 300 m/sec. The V_s in the upper 35 to 45 m of Saugus formation at each site is around 550 to 600 m/sec. The V_s profiles and borehole logs for both sites are published in Gibbs *et al.* (1999); a convenient summary is presented in Figure 4 of Cultrera *et al.* (1999). The V_s profiles in that figure were taken from Gibbs *et al.* (1996), who subsequently revised the profiles in Gibbs *et al.* (1999). The differences in the two sets of profiles are generally small and were found to have no significant effect on the SR analyses in this study.

Forced Vibration Tests and Inertial SSI Models

Vibration Tests

Forced harmonic vibration tests using an eccentric mass shaker provided by the California Institute of Technology were conducted at both buildings in December 1998. The shaker was mounted on the ground floor of the JGB, which was tested first, and then transferred to the third floor (elevation 1305.75 in Fig. 1b) of the JAB. The harmonic shaker force was applied in each principal horizontal direction of each building. The frequency band of excitation was 1.25 to 8.25 Hz, which was the limiting frequency range of the shaker. The weights in the rotating shaker buckets were varied to maintain a maximum shaker force that was in the 4500 to 20,000 N range in this frequency band.

The responses at discrete frequencies during the tests were measured by accelerometers and Ranger seismometers placed at each level of the building. A representative sample of normalized amplitude-response curves is presented in Figure 2. The east–west fundamental frequency (6.2 Hz) was identified for the JAB. As previously noted, the east–west direction corresponds to the shorter plan dimension of this rectangular building, which is more flexible in this direction. The fundamental mode at 6.2 Hz involved mostly horizontal translation with some rocking motion; the modal damping ratio was approximately 8.5%. The fundamental frequency in the stiffer north–south direction for this building is beyond 8.25 Hz based on the amplitude-response curves. At this or any other frequency in the 1.25- to 8.25-Hz band, foundation rocking was not observed during north–south harmonic excitation of the JAB. The tests at the JGB did not reveal any natural frequencies in this frequency band, which was not

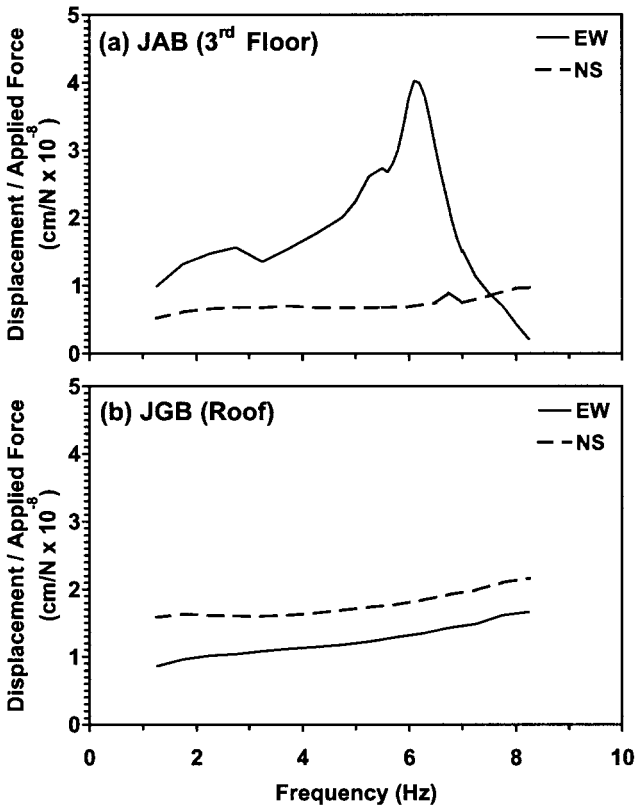

Figure 2. Displacement responses normalized by shaker forces applied during forced vibration tests. Building locations of plotted responses are indicated in parentheses.

surprising given the stiff nature of the building and underlying soils.

Inertial SSI

Inertial SSI models, applicable to small amplitude motions, were developed only for the east–west direction from the vibration-test results. Inertial SSI was not modeled in the north–south direction because no north–south modes of vibration were observed during the vibration tests. The fundamental north–south mode may have appeared in the 5- to 10-Hz band due to the softening of the soil and structure during the MS and AS events, but without a low strain measurement of this frequency, an attempt to estimate and model the inertial SSI in the north–south direction was not judged to be worthwhile.

For the east–west direction, the JGB was modeled as a rigid block with one translational and one rotational (rocking) degrees of freedom (d.o.f.) of the foundation. The JAB was modeled as a three d.o.f. lumped mass-spring system attached to a rigid foundation with the same translational and rocking d.o.f. as in the JGB model. A schematic of this five d.o.f. model can be found in figure 2 of Crouse and McGuire (2001). The SSI models were calibrated as follows. For the JGB, complex-valued dimensionless foundation impedance functions were taken from table 2 of Wong and Luco (1985) for $H/a = 1$. These functions, which apply to a square surface foundation of side length, $2a$, on a uniform viscoelastic layer of thickness, H, over a viscoelastic halfspace, were scaled to the size of the foundation and shear modulus (G) of the 3-m-thick surficial layer. The value of G for this layer was obtained from the V_s survey and was slightly adjusted to yield the same low-frequency translational foundation stiffness as that deduced from the vibration test. The mass and moment of inertia of the block structure were computed from the structural drawings. For the JAB, the masses, moments of inertia, and interstory stiffnesses of the superstructure were estimated from the structural drawings. The foundation stiffnesses were initially estimated from Wong and Luco (1985); however, adjustments to all five model stiffnesses were required to obtain the east–west fundamental frequency and mode shape observed during the vibration tests. The fundamental modal damping ratio was fixed at 8.5% of critical, the same value measured in the vibration test.

Inertial SSI Transfer Functions

The east–west base-to-free-field transfer functions for each building are shown in Figures 3a and 3b, and the building-to-building transfer functions, obtained by dividing the JAB and JGB transfer functions in Figures 3a and 3b, are presented in Figure 3c. Also shown in these figures are the empirical transfer functions derived from the GEOS aftershock motions, which, like the motions generated during the vibration tests, were also not capable of inducing nonlinear response of the SSI system at the JAB or JGB. These empirical transfer functions were computed as the average ratio of

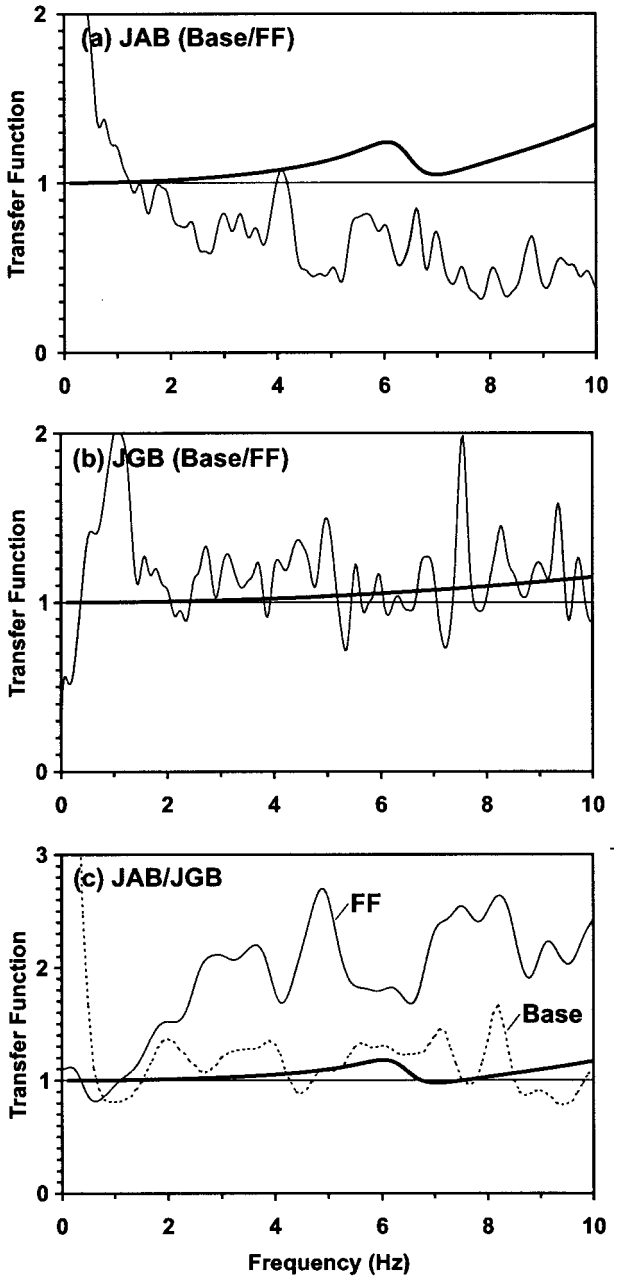

Figure 3. Transfer functions for east–west GEOS records: (a) base-to-free-field motions at the JAB; (b) base-to-free-field motions at the JGB; and (c) JAB-to-JGB motions in the base levels of both buildings and in the free field (FF) at both sites. Thin lines are the empirical functions derived from the records, and the thick lines are the inertial SSI transfer functions calibrated from the vibration-test data.

smoothed versions of the Fourier amplitude spectra (FAS) of the GEOS records. The smoothing was performed with the Hanning spectral window with weights (1/4, 1/2, 1/4) applied 100 times to each FAS, with frequency intervals of 0.035 Hz (MS), 0.019 Hz (AS), and 0.029 Hz (GEOS). The scatter of the ratios about the mean value was reported by

Cultrera *et al.* (1999) for both horizontal components combined into one dataset. Because the dispersion in ratios computed in this study for each component is similar to that of Cultrera *et al.*, this information is omitted in this article to facilitate the comparisons with the theoretical transfer functions. The word "base" in Figure 3 refers to the location within the building where the earthquake motions were recorded (ground floor in the JGB and first floor in the JAB); the abbreviation "FF" means free field. In Figure 3c the corresponding "base" empirical transfer functions were computed as the ratio of the FAS of the in-structure recordings. For reference, this figure also presents a similar ratio for the free-field (FF) recordings at both sites.

Figure 3 clearly demonstrates that inertial SSI is rather modest at the JAB and negligible at the JGB. The empirical JAB transfer function is much less than the theoretical transfer function for frequencies greater than 2 Hz (Fig. 3a), indicating some other SSI phenomenon contributed to this difference. On the other hand, the empirical JGB transfer function oscillates about unity, the general level of the theoretical transfer function (Fig. 3b). The empirical transfer function between the free-field motions (curve FF in Fig. 3c) clearly demonstrates that the JAB free-field motions are greater than the JGB free-field motions, which is apparently due to the amplification of motions through the softer soil at the JAB site. The relative amplification between JAB and JGB is further examined below for the GEOS, AS, and MS records.

Transfer Functions for Free-Field Motions

Site-response (SR) transfer functions between the JAB and JGB free-field motions were estimated using a Windows-based program (ProShake) of the popular SHAKE code (Schnabel *et al.*, 1972), used by Cultrera *et al.* (1999). This program, distributed by EduPro Civil Systems, Inc., Redmond, Washington, was applied to the MS, AS, and GEOS records. The ProShake code models nonlinear site response in an equivalent linear manner by adjusting the shear modulus and material damping ratio for each soil layer to be compatible with the computed shear strain. For this application the motion recorded at the JGB (free field or base) was assumed to equal the free-field motion at a depth of 15 m at the JAB site, with the overlying soil absent (i.e., the JGB motion was assumed to be an outcrop motion at the JAB site).

The JAB soil profile was modeled as shown in figure 4 of Cultrera *et al.* (1999), with the V_s values for each of the five velocity layers taken from figure 24 of Gibbs *et al.* (1996). The fifth layer, with $V_s = 687$ m/sec, was assumed to be the half-space. The outcrop motion was placed at the top of the 3.3-m-thick third layer with $V_s = 456$ m/sec. Shear modulus reduction and material damping curves for "average sand" in the ProShake menu were selected for all layers in the profile. The analysis was repeated using the "upper (bound) sand" curves for all layers. These curves exhibit less nonlinear behavior, but the SR results were virtually identical to those for the "average sand" models subjected to the GEOS and AS motions. Some differences were observed between the "average sand" and "upper sand" results for the MS records. Analyses using the "rock" curves for the underlying layers of the Saugus formation did not affect the results for the MS, AS, and GEOS records.

Three sets of JGB, east–west, and north–south outcrop motions were selected for the analysis: MS building base, AS-1 building base, and AS-4 building base. GEOS records were not required as input outcrop motions because at these small amplitudes, shear modulus and material damping were assumed to be constant; for this linear model the SR transfer function representing the GEOS records was computed directly in ProShake and did not depend on the input motion. For this case, low strain values of shear modulus were computed from the JAB V_s profile, and the damping ratio was selected from the aforementioned "average sand" curve. Each of the four sets of motions (MS, AS-1, AS-4, and GEOS) represents a different order-of-magnitude level of shaking, with the GEOS being lowest and the MS being highest. The AS-1 record is representative of the three strong AS motions (AS-1, AS-3, AS-7), while the AS-4 record is representative of the weak AS motions (AS-2, AS-4, AS-6). This division between weak and strong AS motions was selected by Cultrera *et al.* (1999).

The SR transfer functions computed by ProShake, and the corresponding empirical transfer functions, are shown in Figure 4. The ProShake results for the "average sand" models were used to compute these transfer functions that are displayed in all frames in Figure 4. The bottom frames also show the MS transfer functions computed for the "upper sand" model. The left and right columns of plots in Figure 4 present the results for the east–west and north–south directions, respectively, while the top, upper middle, lower middle, and bottom rows of plots are for the GEOS, weak AS, strong AS, and MS records, respectively. The empirical free-field JAB/JGB transfer functions (FF in Fig. 4a and e) represent the only measure of site response not affected by some form of SSI. For this case, the SR transfer functions are significantly lower than the empirical functions. This lack of agreement is somewhat disconcerting for these low levels of shaking in which the soil behavior is expected to be linear. While better agreement between the SR transfer functions and the empirical functions from the GEOS FF records would have provided more confidence in the SR results for the AS and MS, the possibility exists that the GEOS motions at JGB were not representative of the JAB free-field motions at 15-m depth. This uncertainty could have been eliminated with free-field surface and downhole recordings of the MS and aftershock sequences at both sites.

The middle two rows of plots in Figure 4 deserve additional explanation and discussion. An empirical transfer function is presented as a thin dashed line for each of the three AS records, and the average of the three functions is shown as a short thick dashed line. The SR transfer functions

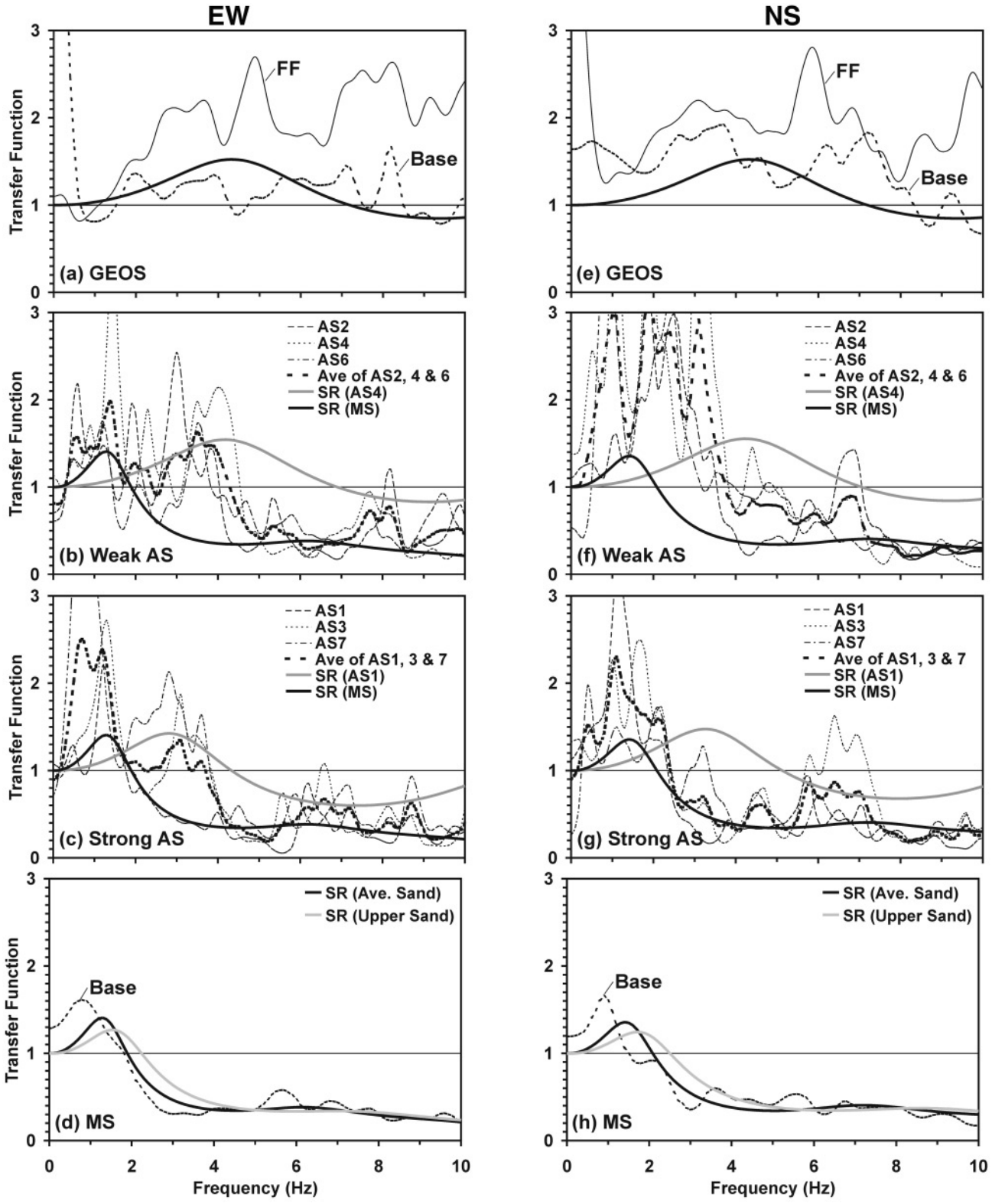

Figure 4. Comparison of empirical transfer functions (thin solid and dashed lines) for GEOS, AS, and MS records and SR transfer functions (thick solid lines) derived from ProShake. Lines labeled FF and Base in first row of plots are the average empirical transfer functions for the free-field and base-level motions, respectively. Thick dashed lines in the middle two rows of plots are the average empirical transfer functions, and the records in parentheses next to SR in the legends of the same plots identify the JGB input outcrop record. In the bottom row of plots, the modulus reduction and damping ratio curves are indicated in parentheses after the SR.

for the MS and representative AS records are shown as thick solid black and gray lines, respectively. The SR transfer function for the MS is shown because of the possibility raised by Cultrera *et al.* (1999) that elevated pore-water pressures induced in the soft alluvium during the MS did not dissipate during the AS events that immediately followed. Although this hypothesis can be debated because of the uncertain location of the water table (Stewart *et al.*, 1996; Woodward-Clyde, 1996; C. Davis, 2001, e-mail comm.), the striking similarity in the empirical transfer functions for the MS and first aftershock (AS-1) suggests some residual effect. For the subsequent strong and weak AS motions, the increase in the amplification and increase in the frequency band over which the amplification is observed indicates the soil began to return to its original state.

As expected, the peaks in SR transfer functions in Figure 4 occur at progressively lower frequencies as the shaking level increases. Beyond the peak frequencies the transfer functions eventually become less than unity, suggesting that the softer surficial soils at the JAB site effectively acted as an isolation device. This filtering is observed in the empirical transfer functions in the 2- to 10-Hz band during the strong MS shaking. In this band, the "average sand" and "upper sand" transfer functions computed by ProShake predict a large reduction in the motions at JAB similar to the observations (Fig. 4d and h). The "average sand" transfer function in these two plots are in closer agreement with the empirical transfer functions; without the benefit of the free-field GEOS database, nonlinear SR could have been easily promoted as the sole reason for the observed differences in the empirical "base" transfer functions among the GEOS, AS, and MS recordings.

Kinematic SSI

Another mechanism that produces filtering of high-frequency motions at the base level of buildings is kinematic SSI (Luco and Wong, 1986; Veletsos *et al.*, 1997). The frequency at which this filtering begins is inversely related to the plan area of the foundation and directly related to the V_s of the underlying medium. Kim and Stewart (2003) developed a simple procedure to estimate base-to-free-field transfer functions that account for kinematic SSI. Their method was calibrated with a large number of strong-motion data recorded during California earthquakes. To implement the method, two shear-wave velocities are required: a low strain value obtained from geophysical surveys (V_s), and a value compatible with the soil shear strain induced during the earthquake ($V_{s,r}$). Each velocity is an average value over a depth equal to the equivalent radius of the foundation and is computed as this depth divided by the time for a vertically propagating shear wave to travel from this point to the ground surface.

Figure 5 presents the kinematic transfer functions for the JAB and JGB for various values of $V_{s,r}$ (listed in the plots)

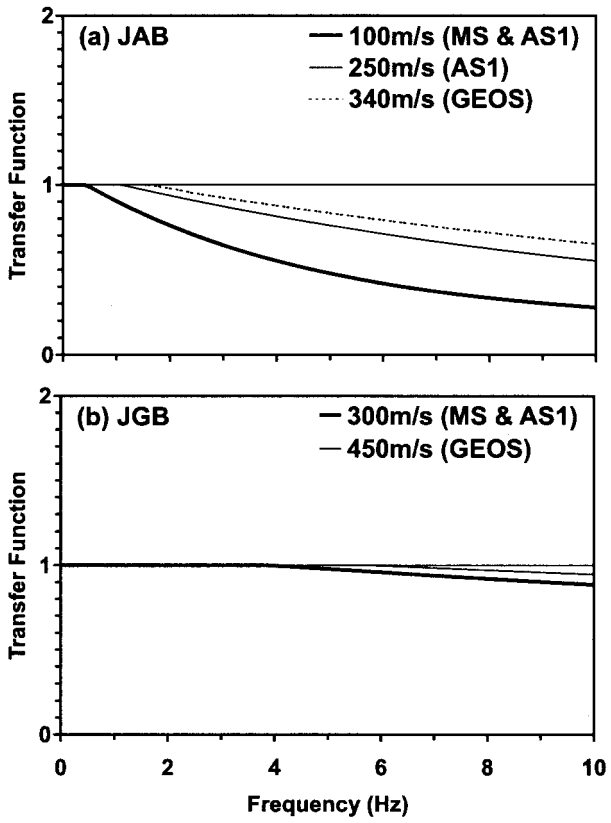

Figure 5. Kinematic SSI transfer functions. Values of reduced shear-wave velocities, $V_{s,r}$, shown in legends.

that were judged to span the range of velocities during the MS, AS, and GEOS events. The velocities for the MS and AS were selected based on the velocity profiles computed by ProShake for maximum shear strains induced by the MS and AS records. Although the ProShake results indicated $V_{s,r}$ = 250 m/sec was appropriate for the JAB AS events, the JAB MS value of 100 m/sec was also used as a lower bound for the AS events because of the previously noted possibility that the pore-water pressures induced at the JAB during the MS did not appreciably dissipate during the AS events. As expected, Figure 5 demonstrates that the effects of kinematic SSI are negligible for the JGB and significant for the JAB. The amount of filtering increases as the $V_{s,r}$ decreases, consistent to some extent with the empirical SR transfer functions in Figure 4.

Composite Transfer Functions

The inertial and kinematic SSI and the SR transfer functions were combined to generate JAB/JGB transfer functions for base response in order to directly compare these functions with their empirical counterparts for the MS, AS, and GEOS events. The potential limitation of such an approach for nonlinear systems is recognized, as the responses of the

JAB structure and underlying soil were certainly nonlinear during the MS and probably during the immediate AS sequence also. However, the transfer functions are intended to provide some insights on the relative contributions of the various effects examined in the previous sections. These functions are assumed to provide reasonable approximations provided adjustments are made to the stiffnesses of the structure and underlying soil. In this regard, the stiffnesses of the low strain inertial EW-direction SSI model for the JAB were reduced by 50% to approximate the behavior at large strains. This reduction was assumed to apply to the MS and AS events. Admittedly, the selection of 50% reduction is somewhat arbitrary, but much smaller reductions would be inconsistent with the large levels of shaking, and much larger reductions would be inconsistent with the lack of damage to the structure and foundation. The issue is not that important because the composite transfer functions are not greatly influenced by inertial SSI, as previously noted.

SSI Transfer Functions

The first set of composite transfer functions were computed by combining the inertial and kinematic transfer functions to produce exclusively EW-direction SSI transfer functions. These functions are shown along with the empirical transfer functions in the left column of plots in Figure 6. The kinematic SSI transfer functions are presented along with the NS-direction empirical transfer functions in the right column of plots in the same figure. In the AS plots, the SSI transfer functions are presented for two values of $V_{s,r}$ that were judged to bound the range of values for these events. The SSI transfer functions show some similarity to the empirical transfer functions at frequencies greater than about 4 Hz for the AS and MS motions. However, differences are readily apparent at lower frequencies and for the NS GEOS motions at all frequencies.

SSI and SR Transfer Functions

The second set of composite transfer functions (Fig. 7) combined the SSI (kinematic and/or inertial) transfer functions from Figure 6 with the SR transfer functions (Fig. 4). The organization of the plots in this figure is similar to that in Figure 6. The inclusion of site response clearly improves agreement between the theoretical and empirical transfer functions, but differences are still observed in some plots. Generally, the average empirical transfer functions in the four AS plots of Figure 7 fall within the two theoretical (SSI + SR) composite transfer functions that were judged to be lower and upper bounds. The empirical MS transfer functions (Fig. 7d and h) are somewhat greater than the theoretical transfer functions. Interestingly, the empirical GEOS transfer function in the NS direction is much greater than the theoretical transfer function; however, in the EW direction, the empirical and theoretical transfer functions for MS and GEOS are generally similar.

Discussion

An examination of the results of the various comparisons indicate that SR and SSI both contributed to the differences observed in the JAB and JGB records. Furthermore, nonlinear soil behavior was clearly important, as noted by Cultrera *et al.* (1999) and affected both phenomena. The degree of similarity between the theoretical and empirical transfer functions in Figure 7 could not have been achieved without incorporating this nonlinear effect approximately in the models used in the analyses.

The obvious effects of kinematic SSI, apparent in the GEOS records from JAB, emphasize the importance of siting ground-motion instruments in true free-field installations or in low rise buildings with small plan dimensions, such as the JGB. Nevertheless, this effect can be potentially significant in small buildings at frequencies higher than the 10-Hz limit of this study, especially if these buildings are founded on soft soils prone to severe degradation during strong shaking. In this case, the soil itself will act as a high-frequency filter, such as inferred from the AS and MS records at the JAB. However, the relative importance of kinematic SSI and nonlinear soil response could have been better isolated in these records if free-field instruments had been installed at both buildings prior to the MS event. Admittedly, the installation of free-field instruments in all desired locations within urban environments is not practical because of vandalism and other perils. Nevertheless, the example of the JAB indicates that kinematic SSI was not fully appreciated or understood when the strong motion instrument was placed in this building. The amount of weak, moderate, and strong motions that the JFP has experienced since 1970, and the nature of the soils, suggest this site should be more fully instrumented with (1) downhole accelerographs, (2) free-field ground-surface accelerographs placed at several locations around the JAB, and (3) a dense array of accelerometers within the JAB. In 2001, permanent downhole accelerometers were installed in two boreholes, one outside the JAB and the other outside the JGB (Steidl and Archuleta, 2002). If the other instrumentation were installed, then more site investigations to better understand the spatial variability of the subsurface stratigraphy and associated soil properties are recommended. Such investigations, particularly at other locations near the JAB, might have resulted in improved site response models.

Acknowledgments

Ben Hushmand and Raul Relles performed the forced vibration tests. Their diligent work and the assistance from Metropolitan Water District personnel at the JFP were greatly appreciated. Ms. Giovanna Cultrera gratefully provided the strong-motion data. Written comments from Dave Boore and an anonymous reviewer led to improvement in the manuscript. Beneficial discussions with Jamie Steidl on the JFP instrumentation are also acknowledged. This study was supported by grants from the National Science Foundation (Grant Nos. 9714858 and 9815053) and U.S. Geological Survey (Grant No. 99HQGR0044).

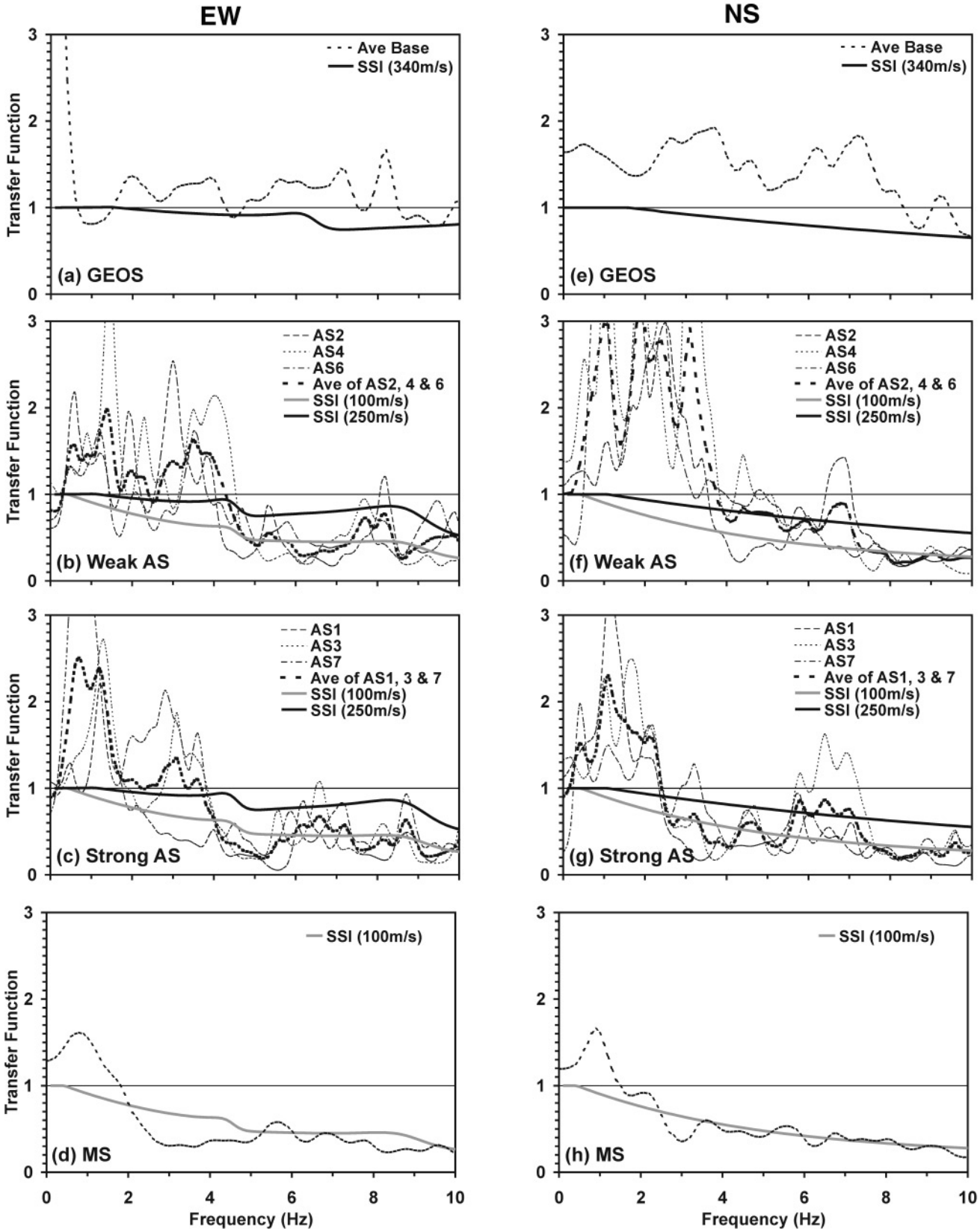

Figure 6. Comparison of empirical transfer functions from Figure 4 and SSI transfer functions (thick solid lines). Combined inertial-kimematic SSI transfer functions are shown for EW direction; only kinematics SSI transfer functions are shown for NS direction. Values of $V_{s,r}$, for JAB are listed in parentheses after SSI in legends.

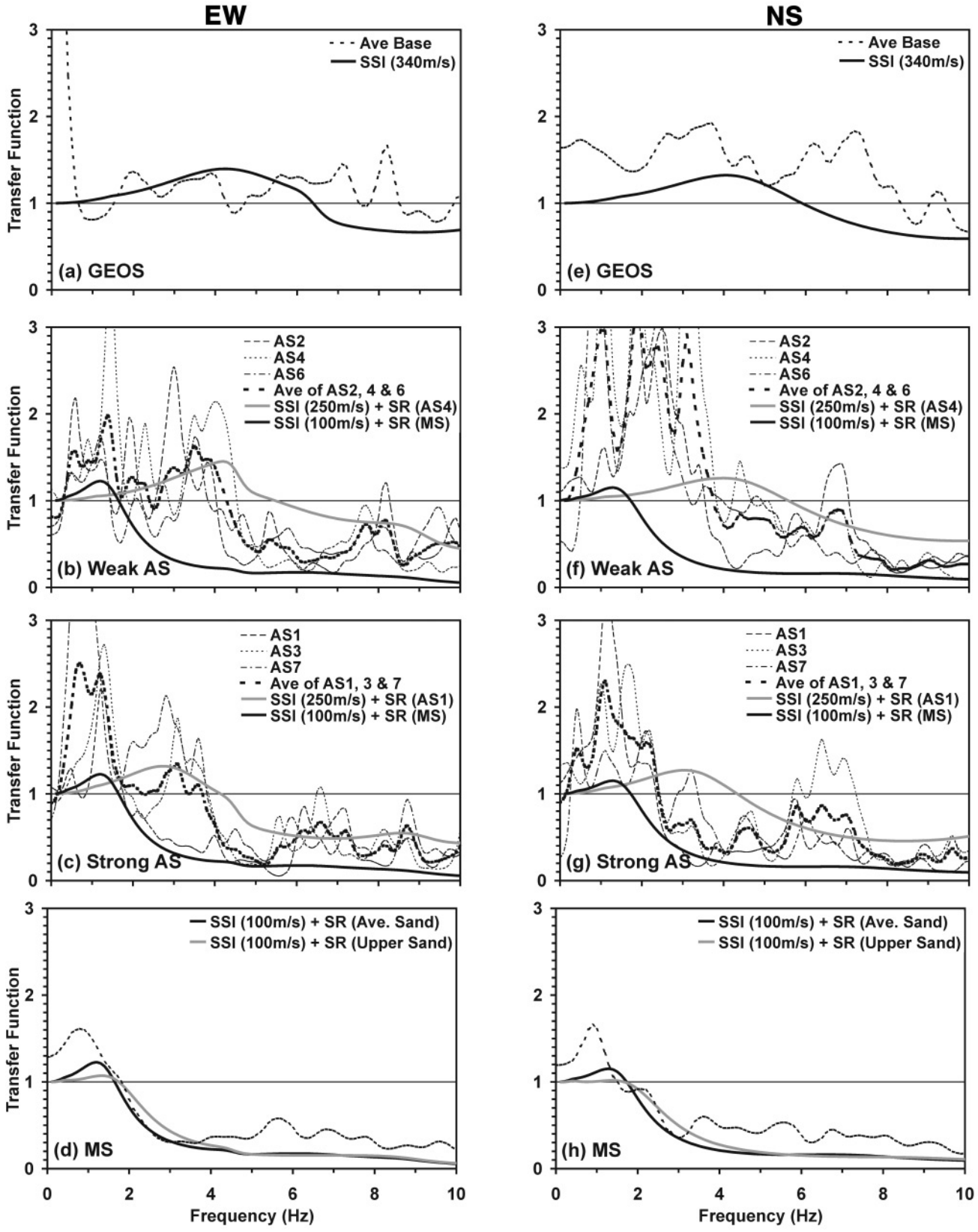

Figure 7. Comparison of empirical transfer functions from Figure 4 and composite SSI-SR transfer functions (thick solid lines). In the legends, values of $V_{s,r}$ for JAB are listed in parentheses next to SSI, and JGB input outcrop record is listed in parentheses next to SR for the weak and strong AS. For the MS plots the modulus reduction and damping ratio curves are indicated in parentheses after the SR in the legend. The average sand curves were used in the SR for the weak and strong AS.

References

Crouse, C. B., and J. McGuire (2001). Energy dissipation in soil-structure interaction, *Earthquake Spectra* **17,** 235–259.

Cultrera, G., D. M. Boore, W. B. Joyner, and C. M. Dietel (1999). Nonlinear soil response in the vicinity of the Van Norman complex following the 1994 Northridge, California, earthquake, *Bull. Seism. Soc. Am.* **89,** 1214–1231.

Gibbs, J. F., J. C. Tinsley, and W. B. Joyner (1996). Seismic velocities and geologic conditions at twelve sites subjected to strong ground motion in the 1994 Northridge, California earthquake, *U.S. Geol. Surv. Open-File Rept. 97-740*, 103 pp.

Gibbs, J. F., J. C. Tinsley, D. M. Boore, and W. B. Joyner (1999). Seismic velocities and geological conditions at twelve sites subjected to strong ground motion in the 1994 Northridge, California, earthquake: a revision of OFR 96-740, *U.S. Geol. Surv. Open-File Rept. 99-446*, 142 pp.

Kim, S., and J. P. Stewart (2003). Kinematic soil-structure interaction from strong motion recordings, *J. Geotech. & Geoenv. Eng. Div. ASCE* **129** (in press).

Luco, J. E., and H. L. Wong (1986). Response of a rigid foundation to a spatially random ground motions, *J. Eng. Mech. ASCE*, **113,** no. 2, 1–15.

Schnabel, P. B., J. Lysmer, and H. B. Seed (1972). SHAKE: A computer program for earthquake dynamic analysis of horizontally layered sites, Report No. EERC 72-12, Earthquake Engineering Research Center, University of California, Berkeley.

Steidl, J., and R. Archuleta (2002). SCEC borehole instrumentation program, *Proceedings and Abstracts of 2002 Southern California Earthquake Center Annual Meeting*, Oxnard, California, 133–134.

Stewart, J. P., R. B. Seed, and J. D. Bray (1996). Incidents of ground failure from the 1994 Northridge earthquake, *Bull. Seism. Soc. Am.* **86,** S300–S318.

Veletsos, A. S., A. M. Prasad, and W. H. Wu (1997). Transfer functions for rigid rectangular foundations, *J. Earthquake Eng. Struct. Dyn.* **26,** 5–17.

Wong, H. L., and J. E. Luco (1985). Tables of impedance functions for square foundations on layered media: *J. Soil Dyn. Earthquake Eng.* **4,** 64–81.

Woodward-Clyde (1996). Site Reconnaissance Following the Northridge Earthquake, January 17, 1994, Appendix D in Geotechnical Investigation, Oxidation Retrofit Program, Jensen Filtration Plant, Granada Hills, California, Prepared for the Metropolitan Water District of Southern California, project No. 934E285A, January 1996.

URS Corporation
1501 4th Avenue, Suite 1400
Seattle, Washington 98101-1616
cb_crouse@urscorp.com
juan_carlos_ramirez@urscorp.com
(C.B.C., J.C.R.)

Manuscript received 10 April 2002.